Contemporary Mathematics
https://ojs.wiserpub.com/index.php/CM/

Research Article

A New Area-Preserving Geometric Numerical Algorithm of Nonlinear Systems

Yunshu Yang[1], Feilong Huang[1], Wenan Jiang[2*], Liqun Chen[1]

[1] School of Mechanics and Engineering Science, Shanghai University, Shanghai, 200444, China
[2] Faculty of Civil Engineering and Mechanics, Jiangsu University, Zhenjiang, 212013, China
E-mail: wajiang@ujs.edu.cn

Received: 20 January 2026; **Revised:** 3 February 2026; **Accepted:** 9 March 2026

Abstract: Geometric numerical integration is a numerical algorithm that preserves the inherent geometric properties of the system. However, most traditional numerical algorithms do not take into account the characteristic, resulting in deviations in some properties during the long-term numerical discretization process. To overcome these issues, advanced numerical algorithms with invariant properties are required. Thus, this work reports the area-preserving performance of the Lie derivative geometric numerical algorithm in the Hamiltonian system. First, we propose a numerical discretization scheme of two-dimensional Hamiltonian systems via the Lie derivative method, and the convergence of the proposed algorithm is demonstrated. Then, the Jacobian matrix of numerical iterative algorithm is implemented, the absolute error, the mean squared error and the cumulative total error of area mapping are derived, respectively. Four criteria of the algorithm for area preservation are given. Furthermore, numerical calculation of two examples confirms that the solution errors over long times is quite satisfactory. Moreover, the cat-face mapping is achieved to prove the quantitative area-preserving.

***Keywords*:** Lie derivative, area-preserving, geometric numerical algorithm, cat-face mapping

MSC: 65L05, 34K06, 34K28

1. Introduction

Numerical algorithms are one of the key tools for the advancement of science. In the last some decades, the numerical methods for general differential equations has achieved a certain level of maturity, and high-precision numerical algorithms are developing rapidly [1–3], mainly including Runge-Kutta methods, linear multistep schemes, composition method, splitting methods, and so on. In particular, with the emergence of new differential equation models, traditional numerical algorithms did not consider the geometric property, which often fails to compute the correct physical characteristics. So they are unable to provide satisfactory solutions. Therefore, developing structure preserving algorithms is needed.

Structure preserving algorithm is an important numerical computation method, which can preserve the inherent geometric properties of the dynamical system. Therefore, a number of research devoted to the field [4–7], such as symplectic methods [8–10], symmetric methods [11, 12], Lie group methods [13, 14], variational integrators [15–18], Lie algebra variational integrator [19], Hamel's field variational integrator [20–22]. These methods can preserve certain

DOI: https://doi.org/10.37256/cm.7220269644

geometric properties of the system, such as energy, the first integral, area, volume, and so on. Recently, the Lie derivative method as a new geometric numerical integration algorithm has been applied to the autonomous systems [23–25], chaos synchronization [26], the non-autonomous systems [27–29], time-varying systems in fractional form [30], the aromatic bicomplex [31], the variable mass systems [32] and maintain the geometric structure of the manifold [33]. Existing studies demonstrate that the method produces numerical solutions consistent with exact solutions or Runge-Kutta approximations, while offering advantages in larger time steps [34] and computational efficiency [24, 25]. Furthermore, it can also be applied to the chaotic motion of a multi-dimensional Hamiltonian system [25], the four high-dimensional chaotic nonlinear systems [35], and a four-dimensional reference space representing the Lagrangian variables [36]. However, prior literature has focused primarily on numerical accuracy and computational performance, neglecting the intrinsic geometric structure of dynamical systems, which critically governs global physical characteristics. The area-preserving is an important type of structure-preserving algorithm which can provide visualized quantitative dynamic behavior. It has extensive applications in fields such as signal processing, image processing, and cryptography. Thus, developing area-preserving properties of the algorithm holds significant value.

In this paper, we address the issue of area preservation of the Lie derivatives algorithm. First, we give a discretization numerical scheme of two-dimensional Hamiltonian systems, and then propose four criteria of the algorithm for area preservation. Subsequently, two numerical examples demonstrate the area-preserving performance of the Lie derivative algorithm under the corresponding conditions.

2. Lie derivative algorithm of Hamiltonian system

2.1 *Lie derivative discretization algorithm*

In this section, consider the area-preserving Lie derivative geometric numerical algorithm for the conservative partitioned Hamiltonian system. The mathematical model can be described as

$$\begin{aligned} \dot{p} &= -\frac{\partial H}{\partial q}, \\ \dot{q} &= \frac{\partial H}{\partial p}, \end{aligned} \tag{1}$$

where $H = H(p, q)$ is the Hamiltonian function of the system, q is the generalized displacement, and p denotes the generalized momentum.

And the discretization schemes can be implemented as

$$\begin{aligned} p_{k+1} &= p_k + \sum_{n=1}^{\eta} \frac{h^n}{n!} L^n_{-H_q}(q_k, p_k), \\ q_{k+1} &= q_k + \sum_{n=1}^{\eta} \frac{h^n}{n!} L^n_{H_p}(q_k, p_k), \end{aligned} \tag{2}$$

where h is the step size, η is the order of Lie exponential expansion, and k is the discrete step.

Since the Hamiltonian Eq. (1) is partitioned into two different, separate parts. Hence, the Lie derivative is realized via the following formula

$$L_{H_p}(p_k) = H_p \frac{\partial q}{\partial q} = H_p,$$
$$L_{-H_q}(p_k) = -H_q \frac{\partial p}{\partial p} = -H_q. \tag{3}$$

The higher-order derivatives can be recursively defined as

$$L^n_{H_p}(q_k, p_k) = L_{H_p}(L^{n-1}_{H_p}(q_k, p_k)) + L_{-H_q}(L^{n-1}_{H_p}(q_k, p_k)),$$
$$L^n_{-H_q}(q_k, p_k) = L_{-H_q}(L^{n-1}_{-H_q}(q_k, p_k)) + L_{H_p}(L^{n-1}_{-H_q}(q_k, p_k)). \tag{4}$$

Noth that due to the nonlinearity of the system, higher-order derivatives are no longer derivatives of the variables q and p as in the first-order Lie derivative, but derivatives of the functions, that is,

$$L_{H_p}(y) = H_p \frac{\partial y}{\partial q},$$
$$L_{-H_q}(y) = -H_q \frac{\partial y}{\partial p}, \tag{5}$$

where $y = y(q_k, p_k)$.

2.2 *Convergence for the Lie derivative algorithm*

Suppose the exact solution of the system are $\bar{p}_k$ and $\bar{q}_k$ in integral interval $[t_0, t_{\text{end}}]$, so the approximate solutions at the point $\bar{q}_k$, $\bar{p}_k$ are denoted as $\tilde{p}_{k+1}$ and $\tilde{q}_{k+1}$, which can be obtained by employing the Lie derivative algorithm Eqs. (2) as

$$\tilde{p}_{k+1} = \bar{p}_k + \sum_{n=1}^{\eta} \frac{h^n}{n!} L^n_{-H_q}(\bar{q}_k, \bar{p}_k),$$
$$\tilde{q}_{k+1} = \bar{q}_k + \sum_{n=1}^{\eta} \frac{h^n}{n!} L^n_{H_p}(\bar{q}_k, \bar{p}_k), \tag{6}$$

then the global error is

$$e^p_{k+1} = |\bar{p}_{k+1} - p_{k+1}|$$
$$e^q_{k+1} = |\bar{q}_{k+1} - q_{k+1}| \tag{7}$$

Subtracting Eqs. (2) and (6) into Eq. (7), and use exact solution, so that

$$\begin{aligned} |\bar{p}_{k+1} - p_{k+1}| &\leq |\bar{p}_{k+1} - \tilde{p}_{k+1}| + |\tilde{p}_{k+1} - p_{k+1}| \\ |\bar{q}_{k+1} - q_{k+1}| &\leq |\bar{q}_{k+1} - \tilde{q}_{k+1}| + |\tilde{q}_{k+1} - q_{k+1}| \end{aligned} \tag{8}$$

At the same time, by leveraging the first-order truncated Lipschitz condition, one has

$$\begin{aligned} |\tilde{p}_{k+1} - p_{k+1}| &\leq (1 + hL_p)\,|\tilde{p}_k - p_k| \\ |\tilde{q}_{k+1} - q_{k+1}| &\leq (1 + hL_q)\,|\tilde{q}_k - q_k| \end{aligned} \tag{9}$$

where the L_p and L_q are the corresponding Lipschitz constants of p_{k+1} and q_{k+1} in the first-order Lie exponential truncated.

So we have the crude estimate

$$\begin{aligned} e^p_{k+1} &\leq (1 + hL_p)e^p_k + C^p_{k+1}h^{n+1} \leq e^{hL_p}e^p_n + C^p_{k+1}h^{n+1} \\ e^q_{k+1} &\leq (1 + hL_q)e^q_k + C^q_{k+1}h^{n+1} \leq e^{hL_q}e^q_n + C^q_{k+1}h^{n+1} \end{aligned} \tag{10}$$

where C^p_{k+1} and C^q_{k+1} are the corresponding coefficients of the local truncation error of p_{k+1} and q_{k+1} in the n-order Lie exponential truncated.

Iterating and evaluating the sum, one has

$$\begin{aligned} e^p_{k+1} &\leq (1 + hL_p)^k e^p_1 + \sum_{m=1}^{k+1} (1 + hL_p)^{k+1-m}\,|C^p_m|\,h^{n+1} \leq \tilde{C}_P \max|C^p_m|\,h^n \\ e^q_{k+1} &\leq (1 + hL_q)^k e^q_1 + \sum_{m=1}^{k+1} (1 + hL_q)^{k+1-m}\,|C^q_m|\,h^{n+1} \leq \tilde{C}_q \max|C^p_m|\,h^n \end{aligned} \tag{11}$$

where the constants $\tilde{C}_p$ and $\tilde{C}_q$ depend on the interval size and the Lipschitz constants L_p and L_q.

It is easy to see that when $h \to 0$, the global error $e^{p,\,q}_{k+1} \to 0$. Therefore, the Lie derivative discretization algorithm is convergent.

3. Area preservation

The definition of area preservation is that the phase flow of the Hamiltonian system remains unchanged after a certain mapping transformation. Hence, the area-preserving of a numerical algorithm can be estimated by the value of the determinant of the Jacobian matrix. Then, the discretization schemes of Eqs. (2) can be rewritten in the form

$$\begin{pmatrix} p_{k+1} \\ \\ q_{k+1} \end{pmatrix} = J_k \begin{pmatrix} p_k \\ \\ q_k \end{pmatrix} \tag{12}$$

where J_k is the Jacobian matrix

$$J_k = \frac{\partial(p_{k+1}, q_{k+1})}{\partial(p_k, q_k)} = \begin{pmatrix} \dfrac{\partial p_{k+1}}{\partial p_k} & \dfrac{\partial p_{k+1}}{\partial q_k} \\ \\ \dfrac{\partial q_{k+1}}{\partial p_k} & \dfrac{\partial q_{k+1}}{\partial q_k} \end{pmatrix}.$$

It is worth noting that the Jacobian matrix serves as a tool for representing local linear transformations and can measure the degree of geometric deformation before and after the transformation [4].

Furthermore, the value of the determinant of the Jacobian matrix is

$$\det(J_k) = \left| \frac{\partial(p_{k+1}, q_{k+1})}{\partial(p_k, q_k)} \right| \tag{13}$$

So that we have the following result.

Criterion 1 If the value of Eq. (13) is equal to one, then the Lie derivative numerical algorithm Eqs. (2) exactly preserves the area.

Unfortunately, the Lie derivative numerical algorithm does not possess a strict symplectic structure. It is usually a function that depends on the step size h. In particular, the value of the step size h is selected to be greater than zero and much smaller than 1. Meanwhile, due to the existence of local truncation errors, the value of the determinant cannot always be equal to 1.

Thus, it is interesting to calculate the error at each step, so that the absolute error for every step is defined as

$$\Delta J_k = \det(J_k) - 1 \tag{14}$$

Thus, the following result is obtained.

Criterion 2 If the absolute value of the absolute error Eq. (14) is a higher-order infinitesimal of the step size h, then the Lie derivative numerical algorithm (Eqs. (2)) is a near area-preserving. Intuitively, $\Delta J_k \to 0$, when $h \to 0$. Thus, the discretization Eq. (12) is a near-identity mapping [37].

The absolute error reflects the difference at each step of the calculation process and is a local error. It can show the evolution of each calculated value over time.

Moreover, of greater interest in understanding the accuracy of the numerical algorithm is the error that deviates from the exact value. With this reformulation, the Mean Squared Error (MSE) is achieved in the integral interval $[t_0, t_{\text{end}}]$ with N steps by

$$\text{MSE}(J) = \frac{1}{N} \sum_{k=1}^{N} (\Delta J_k)^2 \tag{15}$$

Therefore, there is the following criterion.

Criterion 3 If the value of the mean squared error Eq. (15) is a higher-order infinitesimal of the step size h, then the Lie derivative numerical algorithm (Eqs. (2)) is nearly area preserving.

The mean square error is the sum of the squares of the differences between the calculated values and the true values. It is possible to quantify the accuracy of the algorithm's calculated values within a certain computing time interval, and it is an important evaluation metric used to assess the performance of data.

In addition, the mapping J_k produces errors in every transformation, which will lead to the accumulation of errors. Therefore, the total error of the mapping will keep increasing. So the cumulative total error of area mapping is calculated as

$$\Lambda = \prod_{i=1}^{N} [\det(J_i)] - 1 \tag{16}$$

Hence, we have the following criterion.

Criterion 4 If the value of the cumulative total error of area mapping Eq. (16) is an infinitesimal of the step size h, then the Lie derivative numerical algorithm (Eqs. (2)) is an approximately area-preserving transformation.

It is worth noting that criterion 2 is a sufficient condition for criterion 3. Criterion 4 is different from criteria 2 and 3. There is no definite connection between it and criteria 2 and 3. However, it can be seen that criterion 4 is determined from a global perspective and has stronger area-preserving performance compared to criteria 2 and 3.

4. Numerical examples

4.1 *The duffing system*

As a first numerical example, consider the Duffing system, which is a cubic nonlinear conservative Hamilton system, and the equation is employed as

$$\ddot{q} + q + \delta q^3 = 0, \tag{17}$$

where the system has the Hamiltonian

$$H(p, q) = \frac{1}{2}p^2 + \frac{1}{2}q^2 + \frac{1}{4}\delta q^4 \tag{18}$$

And the Lie derivative geometric numerical algorithm is

$$\begin{aligned} p_{k+1} &= p_k - h\left(q_k + \delta q_k^3\right) - \frac{h^2}{2} p_k \left(1 + 3\delta q_k^2\right) \\ q_{k+1} &= q_k + h p_k - \frac{h^2}{2}\left(q_k + \delta q_k^3\right) \end{aligned} \tag{19}$$

The Jacobian matrix of Eq. (19) is

$$J_k = \frac{\partial (p_{k+1}, q_{k+1})}{\partial (p_k, q_k)} = \begin{pmatrix} 1 - \frac{h^2}{2} - \frac{3}{2}h^2\delta {q_k}^2 & -h - 3h\delta {q_k}^2 - 3h^2\delta q_k p_k \\ h & 1 - \frac{h^2}{2} - \frac{3}{2}h^2\delta {q_k}^2 \end{pmatrix} \tag{20}$$

Since Eq. (20) is a matrix, the 2-norm is usually adopted as the Lipschitz condition, namely, $L_p = \|J_k\|_2$. Then, the absolute error of the determinant for the area mapping can be deduced as

$$\Delta J_k = 3h^3\delta p_k q_k + \mathrm{O}\left(h^4\right) \tag{21}$$

So the mean squared error of the determinant is

$$\mathrm{MSE}(J) = \frac{1}{N}\sum_{k=1}^{N}\left[3h^3\delta p_k q_k + \mathrm{O}\left(h^4\right)\right]^2 \tag{22}$$

Moreover, the cumulative total error of area mapping for the Duffing system is performed as

$$\Lambda = \prod_{k=1}^{N}\left[3h^3\delta p_k q_k + \mathrm{O}\left(h^4\right) + 1\right] - 1 \tag{23}$$

Since the system is separable, the symplectic Euler method is the simplest symplectic algorithm and has been chosen as the benchmark for comparison. The corresponding discrete algorithm is

$$\begin{aligned} p_{k+1} &= p_k - h\left(q_k + \delta q_k^3\right) \\ q_{k+1} &= q_k + h p_{k+1} \end{aligned} \tag{24}$$

Obviously, the absolute error, the mean squared error and the cumulative total error of area mapping for the Duffing system are all dependent on the step size h and the initial values $q(0)$ and $p(0)$. Therefore, we discussed the effect of the step size h and the initial values on these errors.

Table 1. The mean squared error of the Duffing system for different different initial values and step sizes

h	0.001	0.002	0.004	0.006	0.008	0.01
lg(MSE(J))	-7.3010	-7.0000	-6.6990	-6.5229	-6.3979	-6.3010

Table 1 shows the mean squared error of the Duffing system for five different initial values (($q(0) = 0.1$, $p(0) = 0$), ($q(0) = 0.5$, $p(0) = 0$), ($q(0) = 1.5$, $p(0) = 0$), ($q(0) = 1.5$, $p(0) = 1.5$) and ($q(0) = 0$, $p(0) = 1.5$)) and six different step sizes ($h = 0.001$, 0.002, 0.004, 0.006, 0.008 and 0.01). The different initial values represent different initial displacements and initial velocities in actual physical systems. It is seen that, as the step size increases, the mean squared error increases.

Hence, as the initial values vary, the mean squared error hardly changes. In addition, when the step size is 0.01, the mean squared error is in the order of $10^{-6.3010}$. According to criterion 3, this is a high-order small quantity that is much smaller than 1 and meets the condition of preserving area.

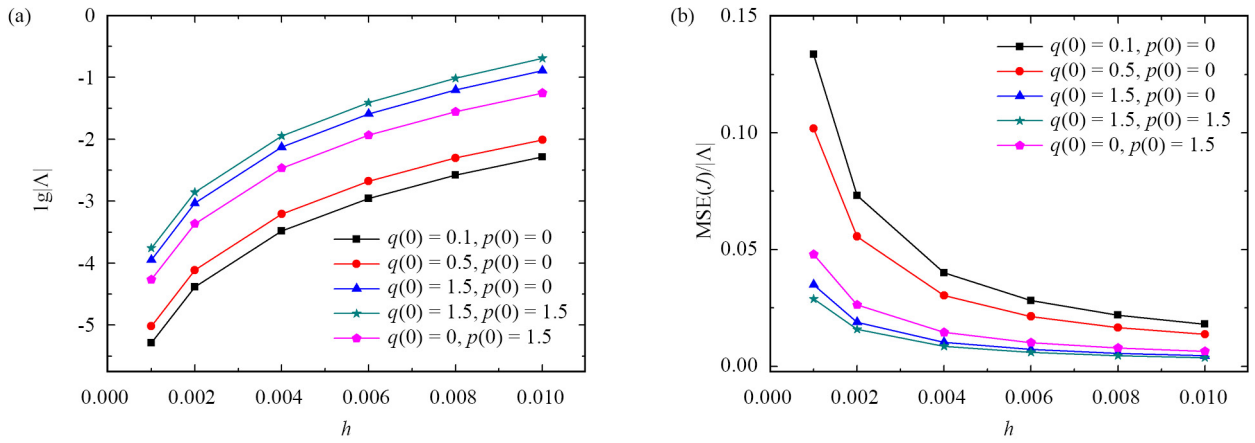

Figure 1. Errors vs step sizes of Duffing system for different initial values: (a) cumulative total error of area mapping, (b) the ratio of the mean squared error to the cumulative total error

Figure 1 displays the logarithmic form of the cumulative total error and the ratio of the mean squared error to the cumulative total error under six different step sizes for different initial values. From the Figure 1(a), we can see that under the same initial value, as the step size increases, the cumulative total error increases. When the initial values are different, but the step size is the same, the cumulative total error fluctuates without any pattern. However, Figure 1(b) illustrates that the ratio of the mean squared error to the cumulative total error decreases with the increase of the step size, and the variation pattern is consistent regardless of the initial values. Meanwhile, as can be seen from Figure 1(b), the mean square error is smaller than the cumulative error. Therefore, the system with a smaller cumulative error has a better area-preserving characteristics. Especially when the step size is small, there is a very small cumulative total error. Thus, a smaller step size has better area-preserving performance.

Furthermore, to check the accuracy of numerical results, the error estimate over long time intervals is plotted in Figures 2 and 3 under two different step sizes $h = 0.01$ and $h = 0.001$. We observe that the absolute error is about 10^{-11} and the cumulative total error of area mapping is about 10^{-5} over long time intervals [0, 20,000] for the step size $h = 0.001$, which satisfies the criteria 2 and 4, and has the property of maintaining area preservation.

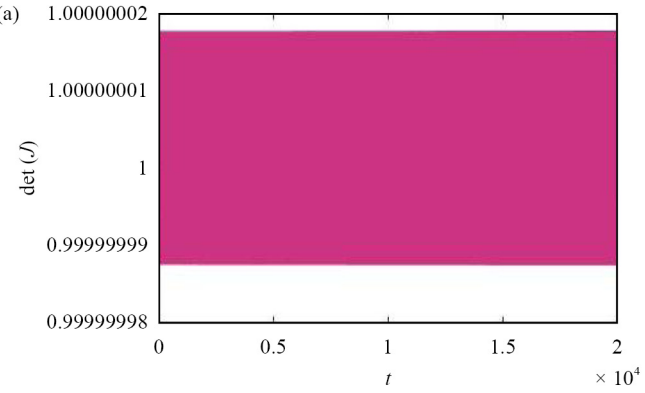

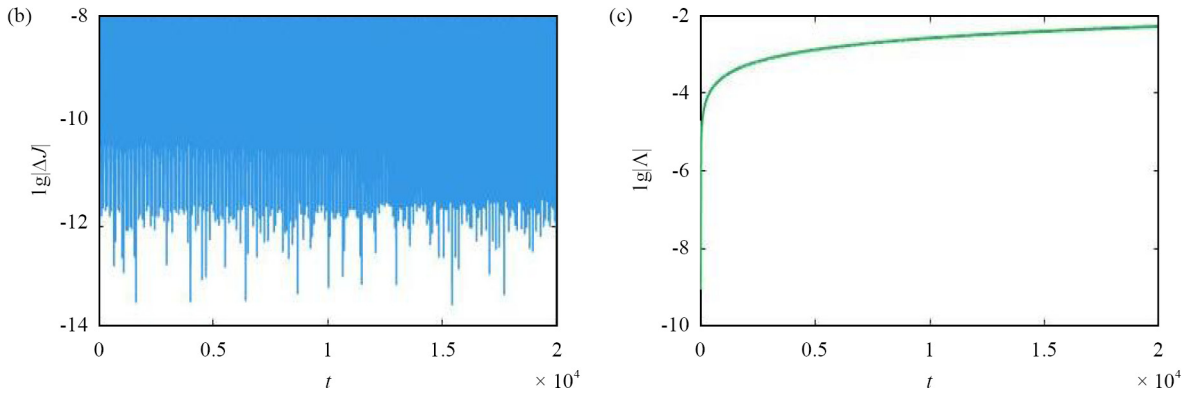

Figure 2. Results of Duffing system over long times with the step size $h = 0.01$: (a) determinant value, (b) absolute error, (c) cumulative total error of area mapping

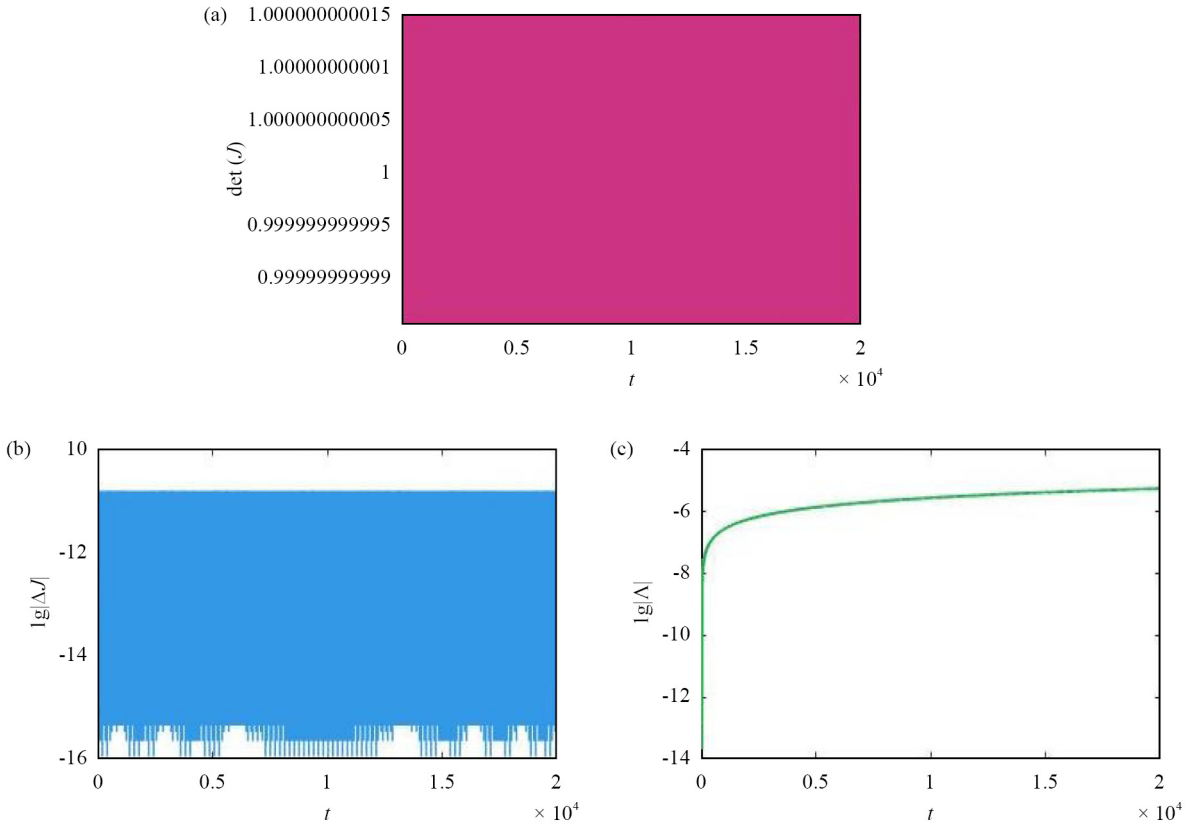

Figure 3. Results of Duffing system over long times with the step size $h = 0.001$: (a) determinant value, (b) absolute error, (c) cumulative total error of area mapping

Moreover, the flow over time is observed by the cat-face mapping. Figures 4 and 5 show the three iterations of exact flow and numerical flow with two different step sizes, where the exact flow is plotted from the invariant Eq. (18), and the numerical flow is computed from the Lie derivative scheme (Eq. (19)), in which the nonlinear coefficient $\delta = 1$ (Its physical meaning is the coefficient of cubic nonlinear restoring force). From these figures, we can see that the exact flow of the system (17) is area-preserving. At the same time, the numerical flow of Lie derivative maintains the dynamic behavior of the exact flow and possesses the geometric property of area preservation.

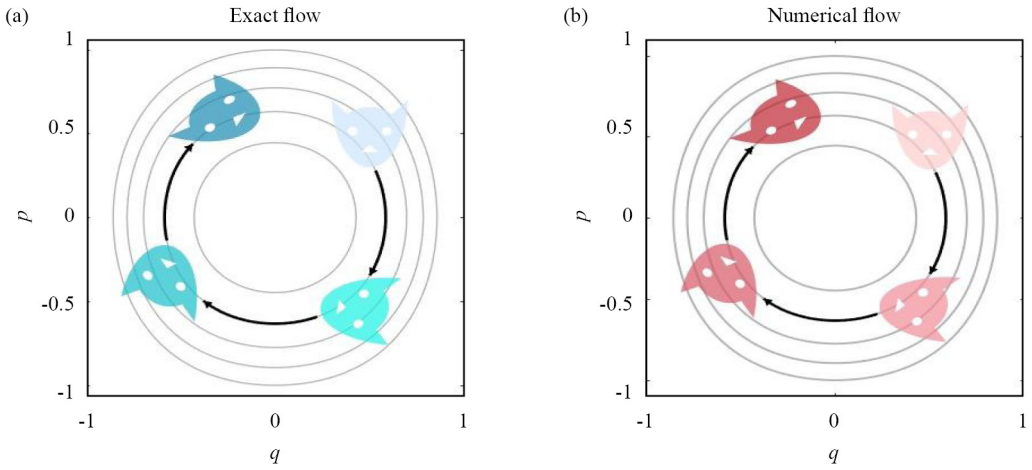

Figure 4. Flow of Duffing system with the step size $h = 0.01$: (a) exact flow, (b) numerical flow

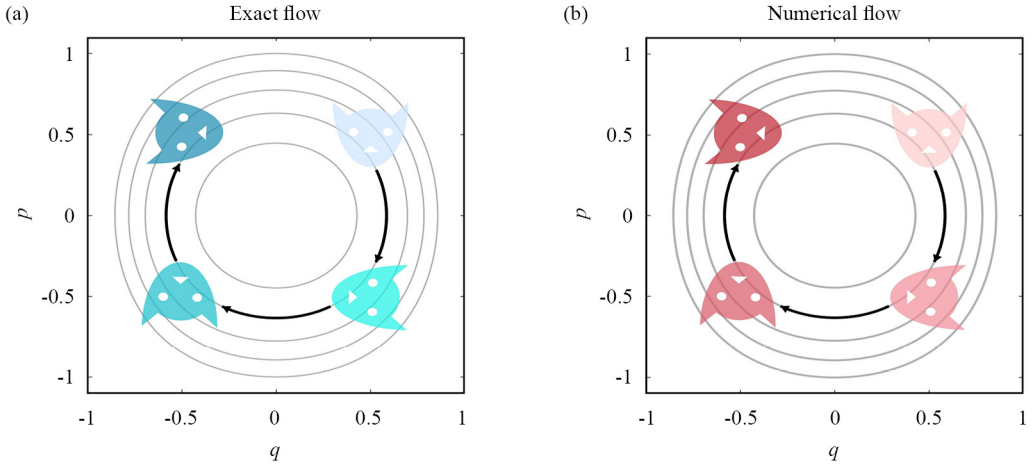

Figure 5. Flow of Duffing system with the step size $h = 0.001$: (a) exact flow, (b) numerical flow

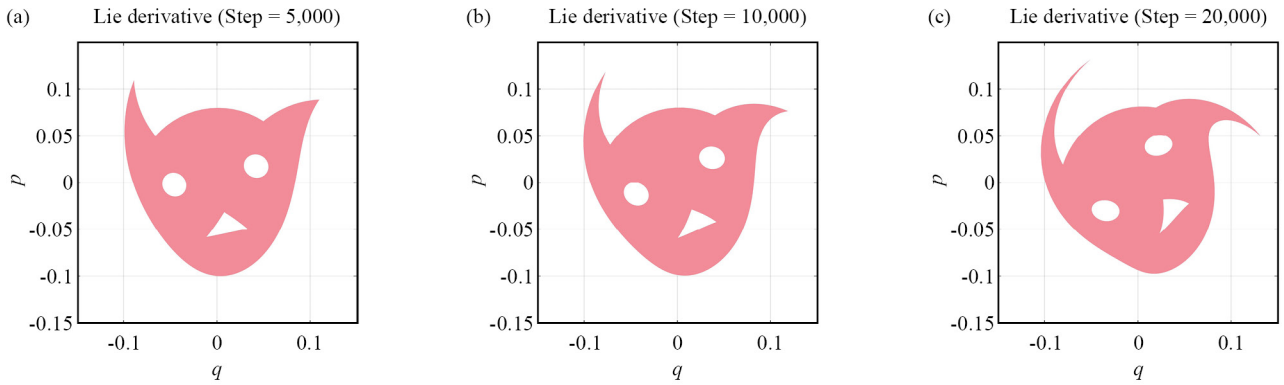

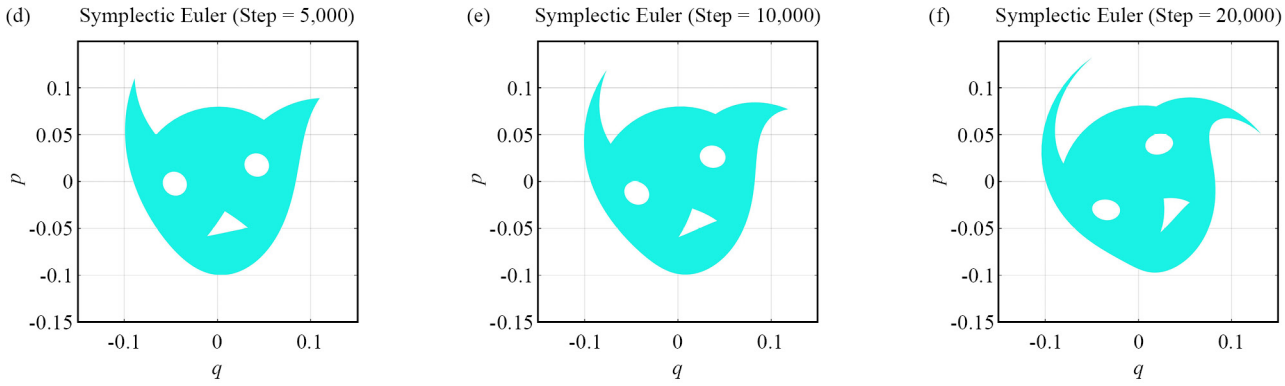

Figure 6. Comparison of flow of the system (17) for multi-step mappings with the step size $h = 0.01$: (a-c) Lie derivative scheme, (d-f) symplectic Euler method

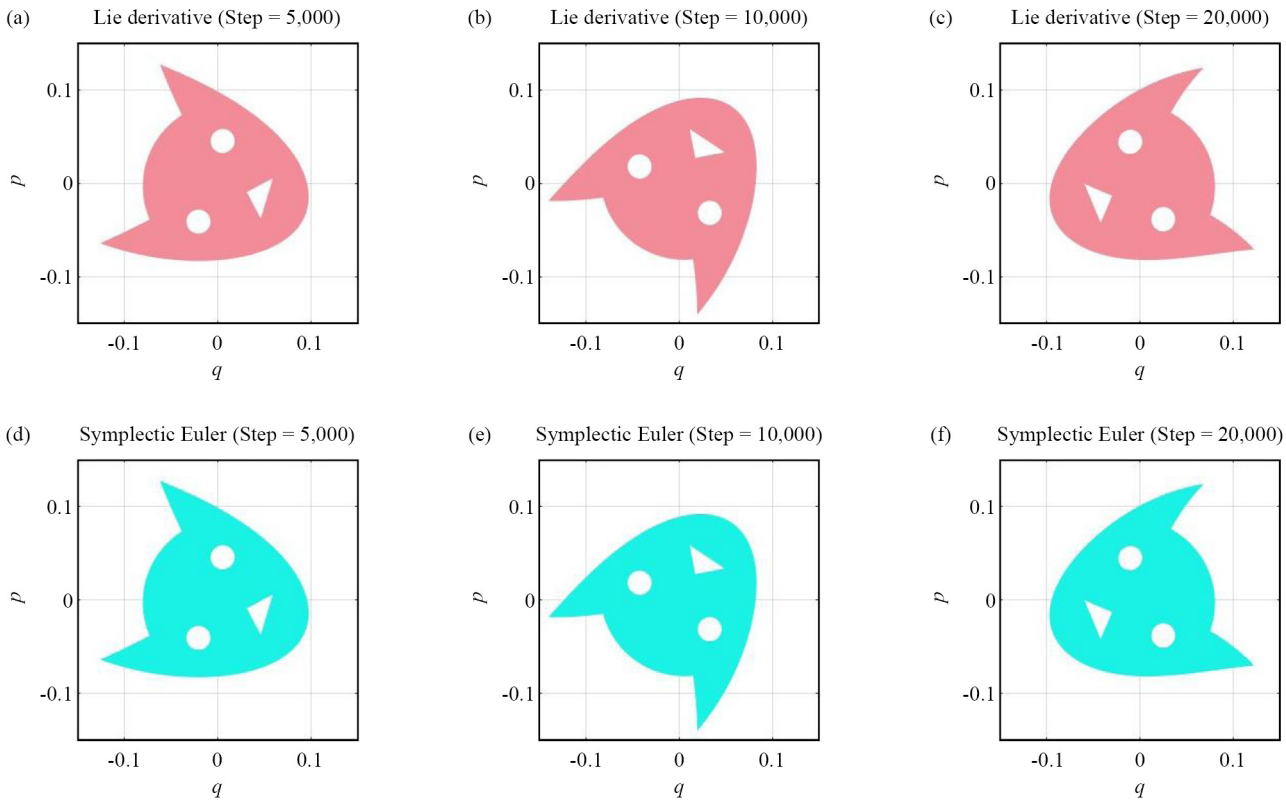

Figure 7. Comparison of flow of the system (17) for multi-step mappings with the step size $h = 0.001$: (a-c) Lie derivative scheme, (d-f) symplectic Euler method

In order to investigate the long-term area-preserving performance of the Lie derivative numerical algorithm, we also calculated multi-step mappings (N = 5,000, 10,000, and 20,000) and compared them with the symplectic Euler method. Figures 6 and 7 show the comparison of the flow of the system (17) for multi-step mappings with two different step sizes. It is seen that the numerical solution obtained from this method is very consistent.

4.2 *The pendulum system*

Let us consider another typical example of a Hamiltonian system, namely, the mathematical pendulum. The differential equation is determined as

$$\ddot{q} + \sin q = 0 \tag{25}$$

where the system has the Hamiltonian

$$H(p, q) = \frac{1}{2}p^2 - \cos q \tag{26}$$

And the Hamilton equations of the system under the proposed discretization numerical scheme are written as

$$\begin{aligned} p_{k+1} &= p_k - h\sin q_k - \frac{h^2}{2}p_k \cos q_k \\ q_{k+1} &= q_k + hp_k - \frac{h^2}{2}\sin q_k \end{aligned} \tag{27}$$

The Jacobian matrix of Eq. (27) is

$$J_k = \begin{pmatrix} 1 - \dfrac{h^2}{2}\cos q_k & -h\cos q_k + \dfrac{h^2}{2}p_k \sin q_k \\ h & 1 - \dfrac{h^2}{2}\cos q_k \end{pmatrix} \tag{28}$$

Then the absolute error of the determinant of the Lie derivative numerical algorithm for the pendulum system is

$$\Delta J_k = \frac{h^4}{4}\cos^2 q_k - \frac{h^3}{2}p_k \sin q_k \tag{29}$$

Similarly, the mean squared error is

$$\mathrm{MSE}(J) = \frac{1}{N}\sum_{k=1}^{N}\left[\frac{h^4}{4}\cos^2 q_k - \frac{h^3}{2}p_k \sin q_k\right]^2 \tag{30}$$

Naturally, the cumulative total error of area mapping is

$$\Lambda = \prod_{k=1}^{N}\left[\frac{h^4}{4}\cos^2 q_k - \frac{h^3}{2}p_k \sin q_k + 1\right] - 1 \tag{31}$$

Similarly, the symplectic Euler method was chosen as the comparison algorithm is

$$\begin{aligned} p_{k+1} &= p_k - h\sin q_k \\ q_{k+1} &= q_k + hp_{k+1} \end{aligned} \tag{32}$$

Note that the errors not only depend on the step size h, but also on p_k and q_k. Then a careful discussion will be considered. Table 2 shows the mean squared error of the pendulum system for different initial values and step sizes. The results shown here have the same characteristics as Table 1.

Table 2. The mean squared error of the pendulum system for different initial values and step sizes

h	0.001	0.002	0.004	0.006	0.008	0.01
lg(MSE(J))	-7.3010	-7.0000	-6.6990	-6.5229	-6.3979	-6.3010

We also plot the cumulative total error of area mapping, the ratio of the mean squared error to the cumulative total error of the the pendulum against the step size in Figure 8, in which the five different initial values are ($q(0) = 0.1$, $p(0) = 0$), ($q(0) = 0.5$, $p(0) = 0$), ($q(0) = 1.5$, $p(0) = 0$), ($q(0) = 1.5$, $p(0) = 1.5$) and ($q(0) = 0$, $p(0) = 1.5$) and the six different step sizes are $h = 0.001$, 0.002, 0.004, 0.006, 0.008 and 0.01). Moreover, Errors of the pendulum over long times are plotted in Figures 9-10 for different step sizes, respectively. As shown in these figures, the proposed Lie derivative scheme gives disappointing error. Meanwhile, the numerical algorithm obtains a considerably satisfactory result over long times.

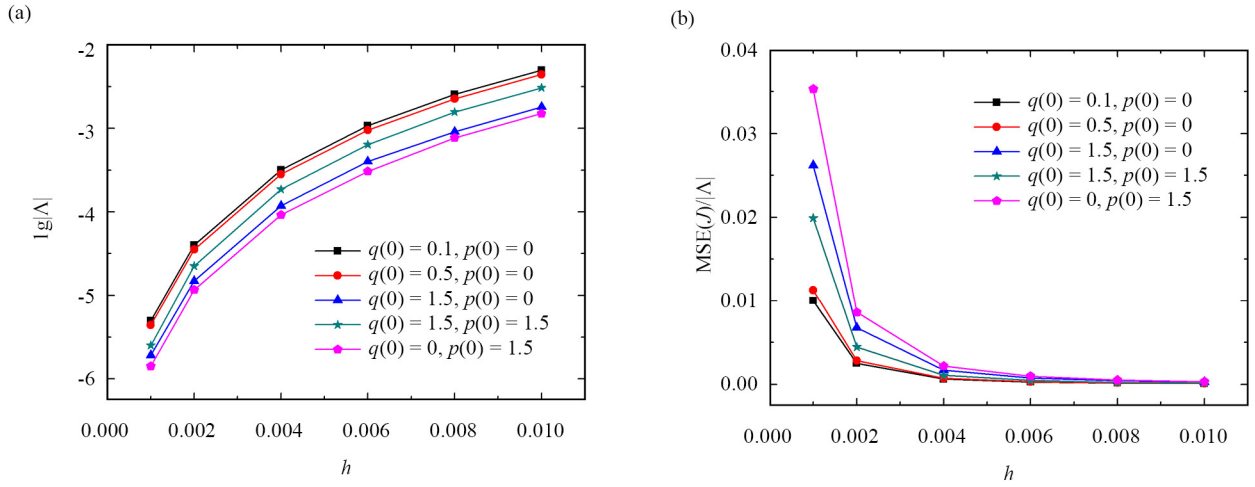

Figure 8. Errors vs step sizes of the pendulum for different initial values: (a) cumulative total error of area mapping, (b) the ratio of the mean squared error to the cumulative total error of area mapping

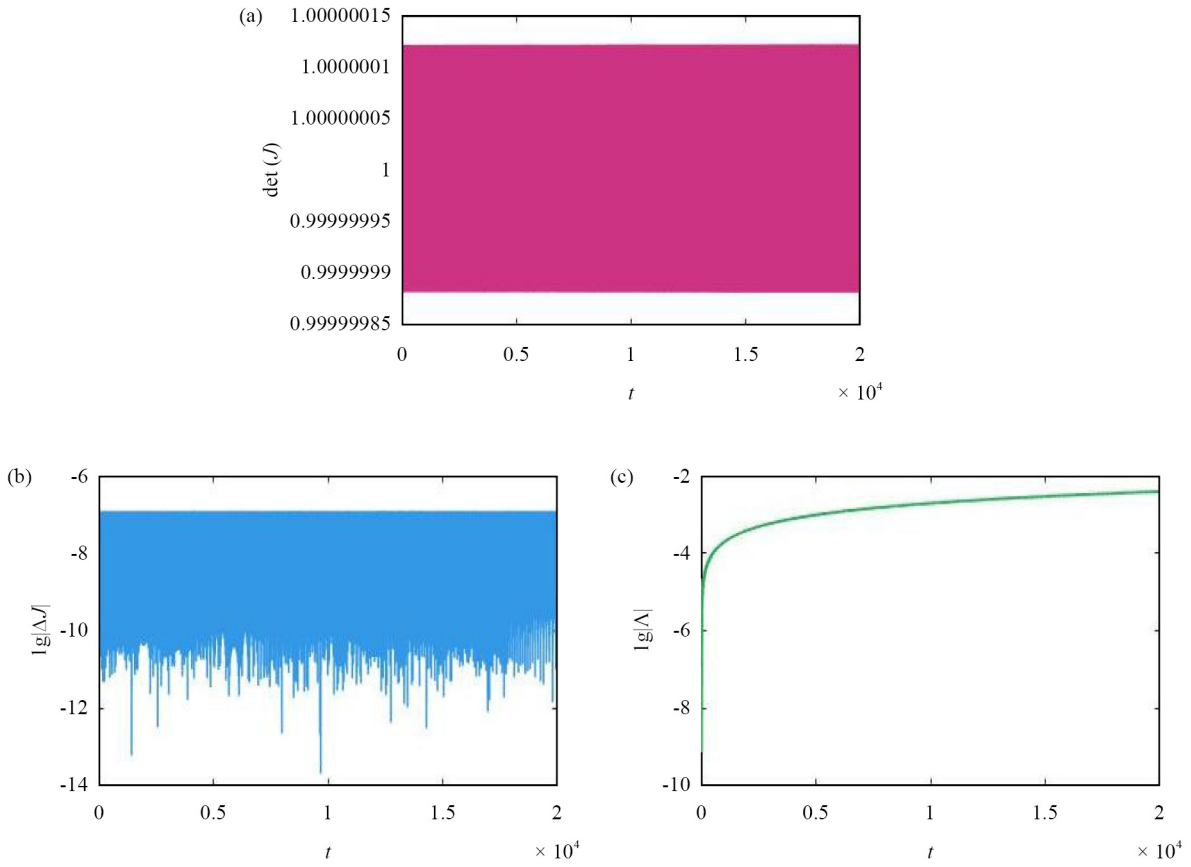

Figure 9. Results of the pendulum over long times with the step size $h = 0.01$: (a) determinant value, (b) absolute error of the determinant, (c) cumulative total error of area mapping

In addition, we also plot the exact flow and numerical flow (see Figure 11 and Figure 12) for the pendulum system with different step sizes, where the exact flow is obtained from the Hamiltonian Eq. (26), and the numerical flow is from the proposed method. Clearly, the flow of both methods almost coincides with each other.

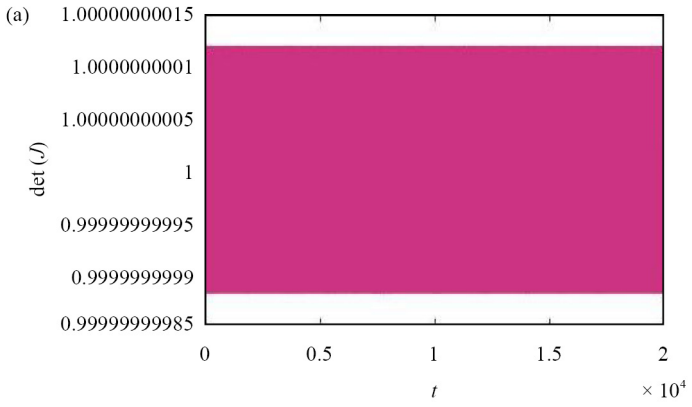

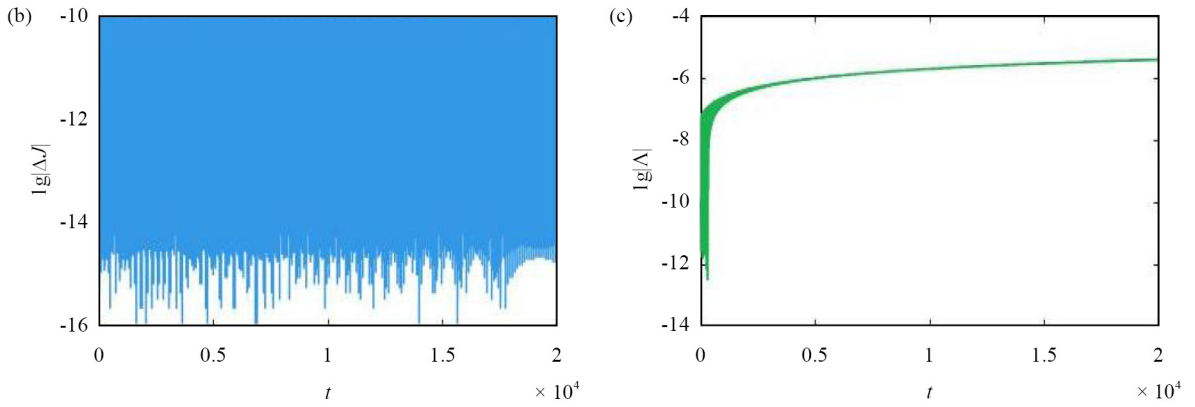

Figure 10. Results of the pendulum over long times with the step size $h = 0.0001$: (a) determinant value, (b) absolute error, (c) cumulative total error of area mapping

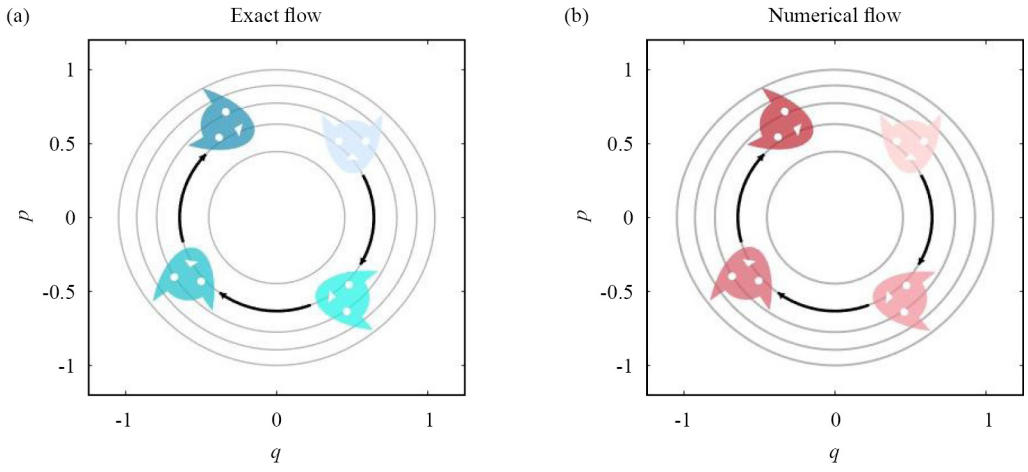

Figure 11. Flow of the pendulum with the step size $h = 0.01$: (a) exact flow, (b) numerical flow

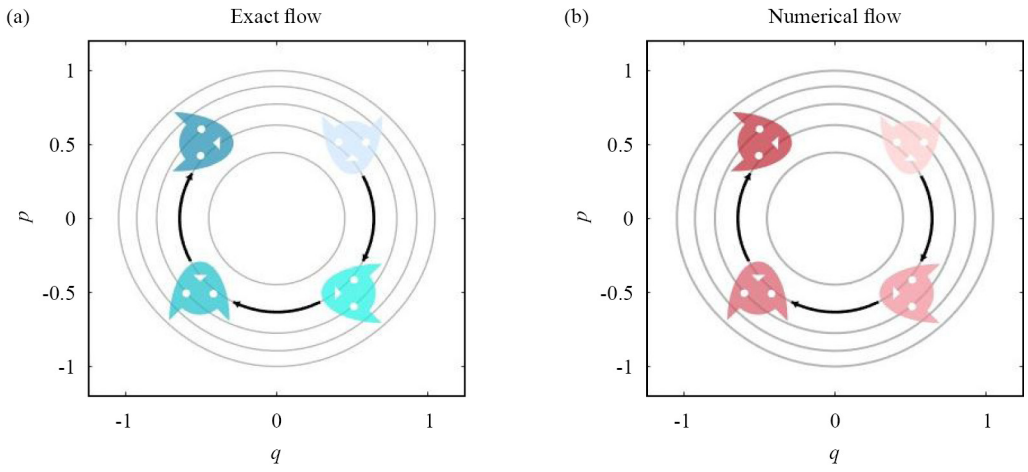

Figure 12. Flow of the pendulum with the step size $h = 0.001$: (a) exact flow, (b) numerical flow

To demonstrate the discussion further, we choose the symplectic Euler method to illustrate the efficiency of the proposed method for multi-step mappings (N = 5,000, 10,000, and 20,000). Figures 13-14 display the variation of the flow calculated by the two numerical methods for multi-step mappings. This is because the symplectic Euler method possesses a strict property of preserving area. It is clear from that the proposed Lie derivative scheme can qualitatively obtain the same results as the symplectic Euler method. Therefore, the Lie derivative geometric numerical algorithm is effective in preserving the area.

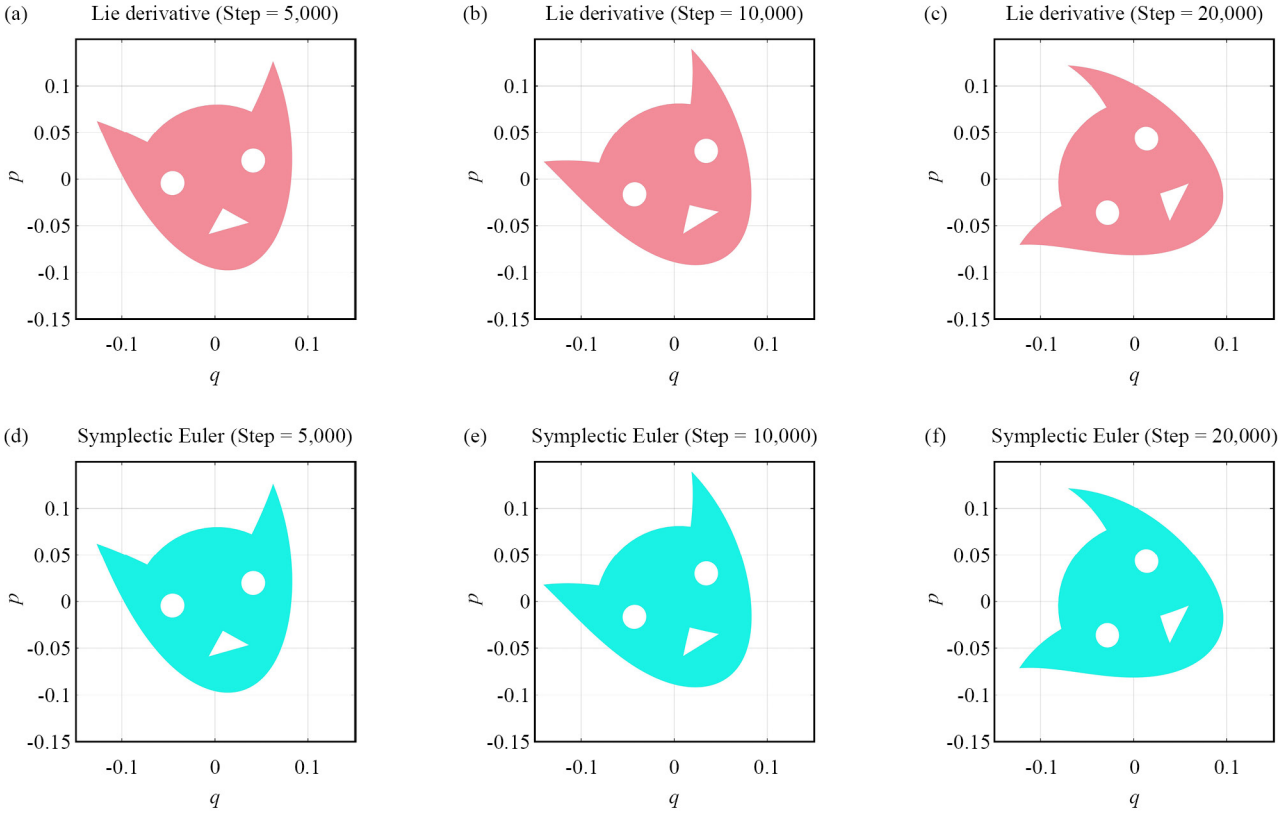

Figure 13. Comparison of flow of the pendulum for multi-step mappings with the step size $h = 0.01$: (a-c) Lie derivative scheme, (d-f) symplectic Euler method

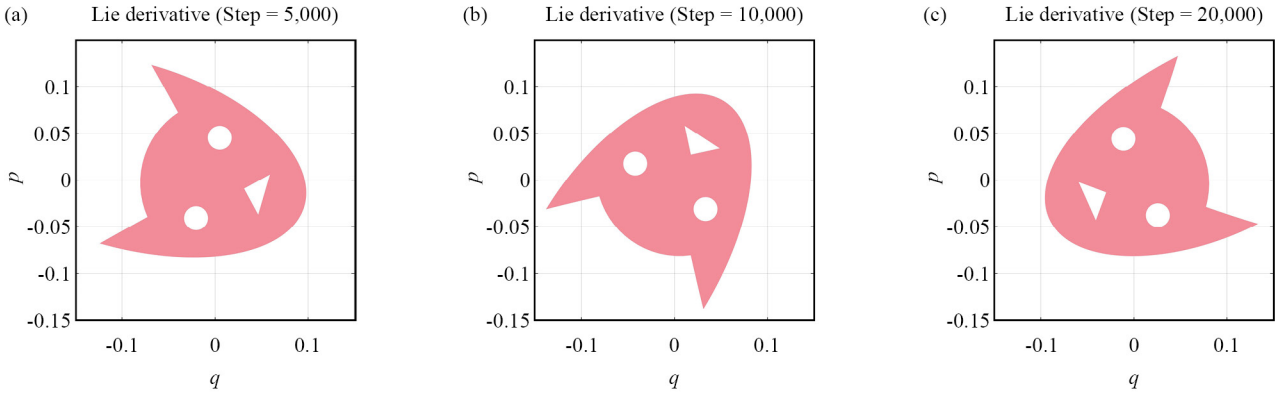

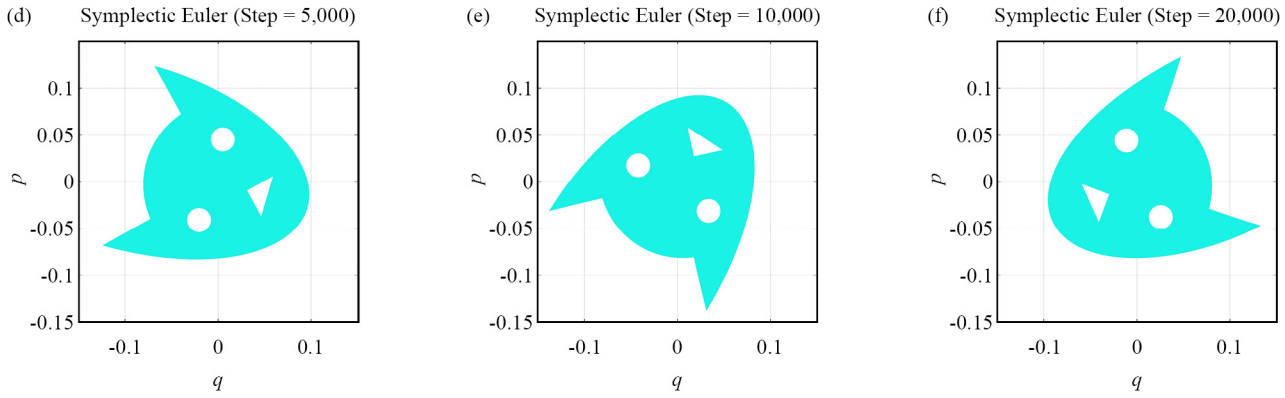

Figure 14. Comparison of flow of the pendulum for multi-step mappings with the step size $h = 0.001$: (a-c) Lie derivative scheme, (d-f) symplectic Euler method

5. Conclusion

This paper proves that the Lie derivative geometric numerical algorithm is for maintaining the area under suitable conditions. And four criteria of the algorithm for area preservation are proposed. The absolute error, the mean squared error, and the cumulative total error of area mapping were calculated by two numerical examples, and the remarkable efficiency of the algorithm were checked. It has been observed that the method preserve the area of cat-face.

Acknowledgement

This paper is supported by the National Natural Science Foundation of China (Nos.12372001 and 12472001), and the authors are grateful to Professor Ernst Hairer from the University of Geneve for providing the cat-face code. The work of Wenan Jiang was supported in part by China Scholarship Council under Grant 202508320415.

Confilict of interest

The authors declare no competing financial interest.

References

[1] Wang B, Zhao X. Geometric two-scale integrators for highly oscillatory system: uniform accuracy and near conservations. *SIAM Journal on Numerical Analysis*. 2023; 61: 1246-1277.

[2] Panda S, Chakraborty S, Hazra B. A general framework for symplectic geometric integration for stochastically excited Hamiltonian systems on manifolds. *International Journal of Non-Linear Mechanics*. 2025; 170: 105001.

[3] Huang H, Zheng Z, Xu Y, Zheng L. A dynamics analysis method for flexible multibody system based on null space symplectic Runge-Kutta algorithm. *International Journal of Non-Linear Mechanics*. 2025; 170: 104999.

[4] Hairer E, Wanner G, Lubich C. *Geometric Numerical Integration: Structure-Preserving Algorithms for Ordinary Differential Equations*. Springer; 2006.

[5] Sharma H, Patil M, Woolsey C. A review of structure-preserving numerical methods for engineering applications. *Computer Methods in Applied Mechanics and Engineering*. 2020; 366: 113067.

[6] Wu XY, Wang B. *Geometric Integrators for Differential Equations with Highly Oscillatory Solutions*. Springer; 2021.

[7] Blanco L, Jimenéz F, de Lucas J, Sardón C. Geometry-preserving numerical methods for physical systems with finite-dimensional Lie algebras. *Journal of Nonlinear Science*. 2024; 34: 26.
[8] Li L, Wang DL. Energy and quadratic invariants preserving methods for Hamiltonian systems with holonomic constraints. *Journal of Computational Mathematics*. 2023; 41: 107-132.
[9] Zhang RL, Liu T, Wang B, Liu J, Tang YF. Structure-preserving algorithm and its error estimate for the relativistic charged-particle dynamics under the strong magnetic field. *Journal of Scientific Computing*. 2024; 100: 70.
[10] Zhang RH, Wang ZX, Xiao JY, Wang F. Structure-preserving algorithms for guiding center dynamics based on the slow manifold of classical Pauli particle. *Plasma Science and Technology*. 2024; 26: 065101.
[11] Hairer E. Symmetric projection methods for differential equations on manifolds. *BIT Numerical Mathematics*. 2000; 40: 726-734.
[12] Zhang TT, Xu MJ. The symmetry-preserving difference schemes and exact solutions of some high-dimensional differential equations. *Applied Mathematics Letters*. 2021; 112: 10681.
[13] Holzinger S, Arnold M, Gerstmayr J. Evaluation and implementation of Lie group integration methods for rigid multibody systems. *Multibody System Dynamics*. 2024; 62: 273-306.
[14] Holzinger S, Arnold M, Gerstmayr J. σ-modified Lie group generalized-α methods for constrained multibody systems. *Mechanism and Machine Theory*. 2025; 217: 106236.
[15] Xia LL, Bai L. Preservation of adiabatic invariants for disturbed Hamiltonian systems under variational discretization. *Acta Mechanica*. 2020; 231: 783-793.
[16] Duruisseaux V, Leok M. Time-adaptive Lagrangian variational integrators for accelerated optimization on manifolds. *Journal of Geometric Mechanics*. 2023; 15(1): 224.
[17] Burby JW, Hirvijoki E, Leok M. Nearly-periodic maps and geometric integration of noncanonical Hamiltonian systems. *Journal of Nonlinear Science*. 2023; 33: 38.
[18] Tran B, Leok M. Multisymplectic Hamiltonian variational integrators. *International Journal of Computer Mathematics*. 2022; 99(1): 113-157.
[19] Chen J, Huang ZH, Tian Q. A multisymplectic Lie algebra variational integrator for flexible multibody dynamics on the special Euclidean group SE(3). *Mechanism and Machine Theory*. 2022; 174: 104918.
[20] Shi DH, Berchenko-Kogan Y, Zenkov DV, Bloch AM. Hamel's formalism for infinite-dimensional mechanical systems. *Journal of Nonlinear Science*. 2017; 27: 241-283.
[21] Shi DH, Zenkov DV, Bloch AM. Hamel's formalism for classical field theories. *Journal of Nonlinear Science*. 2020; 30: 1307-1353.
[22] Chen J, Huang ZH, Tian Q. Hamel's field variational integrator for simulating dynamics of thin-walled geometrically exact beams with warping effects. *Mechanism and Machine Theory*. 2023; 190: 105462.
[23] Monaco S, Normand-Cyrot D. A combinatorial approach of the nonlinear sampling problem. In: *Analysis and Optimization of Systems: Proceedings of the 9th International Conference Antibes*. Springer; 1990. p.788-797.
[24] Mendes EMAM, Billings SA. A note on discretization of nonlinear differential equations. *Chaos*. 2002; 12: 66.
[25] Letellier C, Mendes EMAM, Mickens RE. Nonstandard discretization schemes applied to the conservative Hénon-Heiles system. *International Journal of Bifurcation and Chaos*. 2007; 17(3): 891-902.
[26] Iavernaro F, Mazzia F, Mukhametzhanov MS, Sergeyev YD. Computation of higher order Lie derivatives on the infinity computer. *Journal of Computational and Applied Mathematics*. 2021; 383: 113135.
[27] Zhang XF, Li HQ, Jiang WA, Chen LQ, Bi QS. Exploiting multiple-frequency bursting of a shape memory oscillator. *Chaos, Solitons and Fractals*. 2022; 158: 112000.
[28] Jiang WA, Gu ZH, Liu C, Feng HR, Chen LQ. A high efficiency Lie derivative algorithm for the nonautonomous nonlinear systems. *International Journal of Modern Physics C*. 2023; 34(11): 2350152.
[29] Huang FL, Chen LQ, Jiang WA. A geometric numerical integration with simple cell mapping for global analysis of nonlinear dynamical systems. *International Journal of Bifurcation and Chaos*. 2024; 34(15): 2450190.
[30] Gu ZH, Jiang WA, Chen LQ. Efficient Lie derivative algorithm for two special nonlinear equations. *Pramana-Journal of Physics*. 2024; 98: 114.
[31] Laurent A. The Lie derivative and Noether's theorem on the aromatic bicomplex for the study of volume-preserving numerical integrators. *Axioms*. 2024; 11: 10-22.
[32] Jia XY, Liu C, Jiang WA. Lie derivative discretization scheme for solving variable mass systems. *Journal of the Serbian Society for Computational Mechanics*. 2024; 18: 33-47.

[33] Huang FL, Song YH, Jiang WA, Chen LQ. Lie derivative algorithm for preserving geometry on cylindrical manifolds. *Nonlinear Dynamics*. 2025; 113: 22799-22821.

[34] Mendes E, Letellier C. Displacement in the parameter space versus spurious solution of discretization with large time step. *Journal of Physics A: Mathematical and General*. 2004; 37(4): 1203.

[35] Nepomuceno EG, Mendes EMAM. On the analysis of pseudo-orbits of continuous chaotic nonlinear systems simulated using discretization schemes in a digital computer. *Chaos, Solitons and Fractals*. 2017; 95: 21-32.

[36] Gouin H. Remarks on the Lie derivative in fluid mechanics. *International Journal of Engineering Science*. 2023; 150: 104347.

[37] Duruisseaux V, Burby JW, Tang Q. Approximation of nearly periodic symplectic maps via structure preserving neural networks. *Scientific Reports*. 2023; 13: 8351.